Impact of fuel quantity on luminescence properties of $Sr_3Al_2O_6$:Eu by combustion synthesis

W. T. Barbosa[1,2], C. M. Álvarez-Docio[3], R. Garcia-Carrodeguas[4], M. V. L. Fook[2], M. A. Rodríguez[3], R. E. Rojas-Hernandez[5]*

[1]*University Center SENAI CIMATEC, Salvador, BA, Brazil*

[2]*Federal University of Campina Grande, Academic Unit of Materials Engineering, Campina Grande, PB, Brazil*

[3]*Instituto de Cerámica y Vidrio, Madrid, Spain*

[4]*Noricum S.L., Madrid, Spain*

[5]*Tallinn University of Technology, Department of Mechanical and Industrial Engineering, Tallinn, Estonia*

Abstract

The photoluminescent behavior of Eu-doped $Sr_3Al_2O_6$ obtained by highly efficient solution combustion synthesis is reported. In order to understand the influence of the fuel on the synthesis, the stoichiometric quantity and an excess of fuel were evaluated. By adjusting the amount of fuel, different luminescence responses were obtained, allowing europium cations incorporation into the $Sr_3Al_2O_6$ lattice to serve as effective luminescence activators in such a short time during the rapid combustion synthesis process. The higher amount of fuel in the presence of the oxidizing agent produced $Sr_3Al_2O_6$:Eu particles with higher phosphorescence brightness, owing to the increase of the reduction process from Eu^{3+} to Eu^{2+}. The synthesized phosphor showed an intense band emission centered at 515 nm and could be excited over a broad spectral range in the UV-visible region. Particles having nanostructured flake-type morphology were obtained, which was considered a micro-nanofunctional candidate for practical applications.

Keywords: combustion, aluminate, luminescence.

INTRODUCTION

Phosphors are materials that have the ability to absorb high energy (short wavelength) and down-convert them into lower energy (longer wavelength) [1]. Usually, phosphors are composed of two parts, one part is the lattice and another part is an activator or dopant. Activator ions are the chief luminescent center of the host lattice [2, 3]. The commonly used activators are Eu^{3+}/Eu^{2+}, Ce^{3+}, Tb^{3+}, Gd^{3+}, Yb^{3+}, Dy^{3+}, Sm^{3+}, Tm^{3+}, Er^{3+}, Nd^{3+}, etc. [4]. The luminescence properties of Eu^{2+}-doped strontium aluminates have been widely studied since it has good luminescent properties such as high initial luminescent intensity, long afterglow, good stability, and can reveal broad-band emission because of the electronic transitions between the fundamental state of $4f^7$ and the excited state of $4f^65d^1$ [5, 6]. The rare earth ions act as luminescent centers in strontium aluminates host [7]; these phosphors are known as efficient green and blue emitters, and for their long-persistent luminescence [8].

The undoped $Sr_3Al_2O_6$ material does not show any luminescence but the emission spectra of europium-doped material show luminescence in the wavelength range from 580 to 620 nm. The $Sr_3Al_2O_6$:Eu^{2+} phosphor shows green emission peaking at 538 nm excited at 377 nm with an additional broad band at a longer wavelength. Under lower energy excitation the red emission centered at 625 nm can be observed. Clearly, multiple emission bands/colors can be observed depending on the excitation wavelength. According to structural data, six different strontium sites exist in $Sr_3Al_2O_6$. Therefore, one can expect that substitution of Sr^{2+} sites by Eu^{2+} ions should lead to six different types of luminescent Eu^{2+} centers. The $Sr_3Al_2O_6$:Eu^{3+} phosphor exhibits narrow emission at 580, 592, 595, 613, and 617 nm instead of characteristic 520 nm emission which is the case for divalent europium [6, 9]. The duration of the photoluminescence from a phosphor is affected by a number of parameters such as the type and amount of activators or dopants, the structure of the host lattice, the method of preparation or growth conditions, the particle size and other post-treatments. These parameters play a significant role in inducing a crystal field effect within the host matrix which in turn influences the emission wavelength, intensity, and lifetime [10].

Strontium aluminate can be synthesized by different techniques, such as sol-gel, solid-state, hydrothermal, and combustion methods [11]. Some of these routes require a multi-step process and long calcination treatments at high temperatures to prepare crystalline materials [12] and their heterogeneity is inevitable [13], in addition to a low surface area [14]. Commonly, for large-scale production of luminescent powders, the conventional solid-state reaction process is used [15]. However, this process has the disadvantages previously reported. Currently, solution combustion is being considered a promising approach due to its several advantages, providing a nanostructured powder with high purity, better homogeneity, and high surface area

**willamsteles@yahoo.com.br*

https://orcid.org/0000-0002-3019-3195

in a rapid, inexpensive single-step operation; the materials obtained by this route can be used in different advanced applications, including catalysts, fuel cells, biotechnology, radiation detector, and photoluminescent properties [16-19]. According to Rojas et al. [18], $SrAl_2O_4$ doped with Eu^{2+} and Dy^{3+} are successfully synthesized by the combustion method avoiding thermal treatments in a reducing atmosphere. They established that the amount of urea as a fuel has an important influence on phase composition and determines the presence of an oxidizing agent such as HNO_3 to complete the reaction, when the fuel content employed is greater than the stoichiometric ones.

The objective of this work is to evaluate the effect of the amount of fuel on the properties of $Sr_3Al_2O_6$:Eu synthesized by the solution combustion method. Herein, we describe the effect of stoichiometric quantity and excess fuel on the properties of the $Sr_3Al_2O_6$:Eu. The use of a complementary oxidizing agent could improve the reaction completion, as also influence the microstructural characteristics of the compound. The correlation between the combustion process, morphology, and optical properties of strontium aluminate-based particles is discussed.

EXPERIMENTAL

Procedure: the $Sr_3Al_2O_6$:Eu was prepared by solution combustion synthesis (SCS) method using strontium carbonate ($SrCO_3$, >98%, Cinética Reag. Sol.), europium oxide (Eu_2O_3, 99.5%, Metal Rare Earth), aluminum nitrate [$Al(NO_3)_3.9H_2O$, >98%, Sigma-Aldrich] and nitric acid (HNO_3, 65%, Merck) for the dissolution of the carbonate into nitrate, increasing the oxidizing character of the reaction. These reagents were dissolved in 50 mL of deionized water. The amount of each reagent was calculated according to

$$\begin{aligned}&(3\text{-}x)SrCO_3(s) + 0.015Eu_2O_3(s) + 2Al(NO_3)_3.9H_2O(aq) + \\ &10\varphi(NH_2)_2CO(aq) + [6+(\varphi\text{-}1).12]HNO_3(aq) \rightarrow \\ &Sr_{2.97}Eu_xAl_2O_6(s) + (26\varphi+15)H_2O(g) + \\ &13\varphi CO_2(g) + 16\varphi N_2(g)\end{aligned} \quad (A)$$

with a doping concentration of x=0.03 using the calculation proposed by Jain et al. [20]. Urea [$(NH_2)_2CO$, >99.5%, Sigma-Aldrich] was used as a fuel, in a stoichiometric oxidizing/reducing ratio of 1:1 (φ=1). In the second route, excess urea was tested with a stoichiometric oxidizing/reducing ratio of 1:2 (φ=2), which implied that the amount of fuel was twice as stoichiometric. For all the routes, we looked for the synthesis of 5 g of $Sr_{2.97}Eu_{0.03}Al_2O_6$ powder. For φ=1, the amount of urea required gave a stoichiometric ratio of fuel to oxidant, considering as oxidant only the aluminum nitrate; φ=2 implied that the amount of fuel was twice the stoichiometric one, in this case, the stoichiometric amount of HNO_3 was added to balance the total amount of fuel. The reactant mixtures were partially dried under magnetic stirring for 120 min at 80 ºC in a porcelain crucible, then placed in the furnace at 600 ºC for about 10 min; during this time, ignition took place.

Characterization: the products obtained by SCS were crushed with an agate mortar obtaining a fine powder. For X-ray characterization, this powder was ground in a pulverizing mill (MM2, Retsch, Germany) for 5 min. Identification of crystalline phases in synthesized powders was carried out by X-ray diffraction analysis using a diffractometer (D8, Bruker, Germany) with CuKα radiation (λ=1.5406 Å), working at 40 kV and 40 mA. For the acquisition of the diffractograms, they were recorded in step mode in a range of Bragg angle (θ), scanning angles between 15-60° 2θ, with a step of 0.02° and accumulation time of 4 s. A software (X'Pert HighScore Plus, PANalytical, Netherlands) was used for qualitative phase analysis. The morphology of the nanostructured powders was evaluated using field-emission scanning electron microscopy (FE-SEM, S-4700, Hitachi) with images of secondary electrons. Surface area measurements were performed using a single point isotherm technique (Monosorb Surface Area MS-13, Quantachrome Instr., USA) and applying the Brunauer, Emmett, and Teller (BET) model. The equivalent particle size was calculated based on the BET surface area as follows [21]:

$$D_{BET} = \frac{6}{S_{BET}.\rho} \quad (B)$$

where D_{BET} is the equivalent particle size (μm), S_{BET} (specific surface area), and ϱ (theoretical density of $Sr_3Al_2O_6$ - 3.57 g/cm^3). The optical properties of these materials by measuring emission and excitation spectra were investigated. The photoluminescence spectra of the phosphor particles were recorded with a spectrofluorometer (Fluorolog-3, Horiba Jobin Yvon) at room temperature. The luminescence intensity was measured over the wavelength 260-700 nm; a xenon arc lamp was used as the excitation source (λ_{exc}= 365 and 464 nm), and slits of 2.00 and 10.00 nm bandpass were used for measurements of the emission and excitation spectrum, respectively.

RESULTS AND DISCUSSION

Obtaining powders: solution combustion synthesis consisted of three main steps (Fig. 1), such as: a) homogenization of the precursors by dissolution; b) formation of the gel with the fusion of nitrates; and c) combustion of the gel, obtaining at the end a voluminous and fragile solid. The synthesized products were ground and

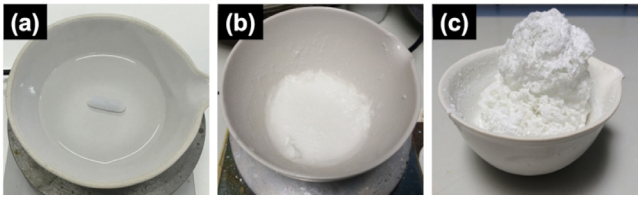

Figure 1: Images for a schematic description of the main steps in solution combustion synthesis (SCS).

characterized by XRD for their phase compositions.

Structural characterization: X-ray diffractograms of phosphors obtained by combustion under stoichiometric urea quantity and with twice the quantity (φ= 1 and 2) are shown in Fig. 2. The results for samples in the stoichiometric amount of urea (φ=1) led mainly to the main formation of the $Sr_3Al_2O_6$ cubic phase, space group Pa3, characterized by three peaks at angles (2θ) of 31.949º, 45.765º and 56.890º accordingly with JCPDS file nº 24-1187 and a minority phase $SrAl_2O_4$ (monoclinic phase) accordingly with JCPDS file nº 34-0379. The presence of crystalline phases having different Sr/Al ratios revealed the lack of homogeneity in the system during the combustion process [18], as could also be related to the proximity between these two phases as can be seen in the equilibrium phase diagram of SrO-Al_2O_3 system according to Hanic et al. [22]. On the other hand, the formation of strontium carbonate may be assigned to high SrO basicity and the presence of CO_2 (slightly acid gas) generated during the combustion [23]. With the excess of fuel (φ=2), the main phases present in stoichiometric synthesis (φ=1) were identified, having as the major phase $Sr_3Al_2O_6$ and $SrAl_2O_4$ as the minor phase. The presence of these phases was again attributed to the characteristic lack of energy homogeneity during the combustion reaction [24]. There was less presence of the strontium carbonate phase, indicating that the increase of oxidant (HNO_3) in equilibrium with the fuel [$(NH_2)_2CO$] resulted in a greater decomposition of $SrCO_3$.

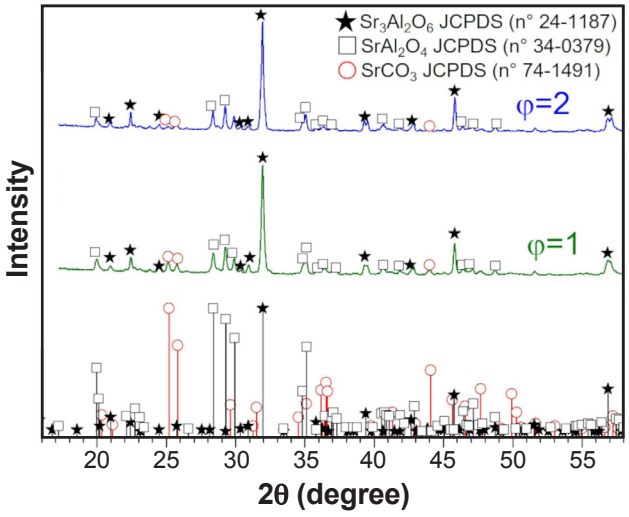

Figure 2: XRD patterns of synthesized $Sr_3Al_2O_6$ phosphors synthesized with the stoichiometric amount of fuel (φ=1) and with excess fuel (φ=2). The symbols highlight $Sr_3Al_2O_6$ (black stars), $SrCO_3$ (open red circles), and $SrAl_2O_4$ (open black squares).

Microstructural characterization: the FE-SEM analysis was carried out to investigate the morphology of synthesized products. FE-SEM images at different (low and high) magnifications have been taken, as shown in Fig. 3. In Figs. 3a and 3d, the morphology of the products is observed (for φ= 1 and 2, respectively); they present a typical synthesis microstructure due to the combustion of the flake form [25] with many voids attributed to the large volume of gases generated during combustion reaction; by analyzing the micrographs in more detail, it was noted that these flakes were nanostructured. In Figs. 3e and 3f,

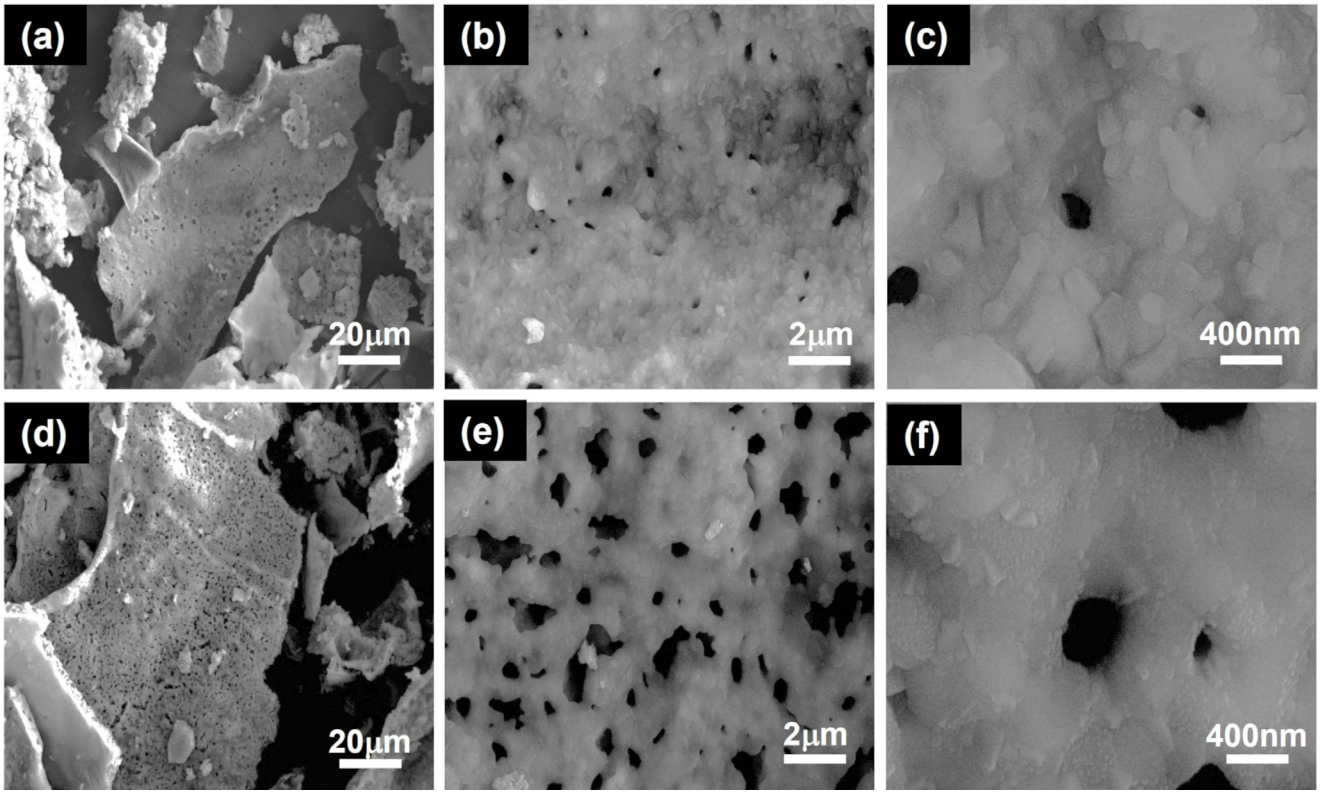

Figure 3: FE-SEM micrographs at different magnifications (low and high) of the products obtained for φ=1 (a,b,c) and φ=2 (d,e,f).

Table I - Dependence of specific surface area (S_{BET}) and equivalent particle size (D_{BET}) on amount of fuel (φ).

Sample	S_{BET} (m^2/g)	D_{BET} (μm)
φ=1	0.15	11.2
φ=2	0.07	24.0

it is observed the morphology of the powder synthesized with excess fuel (φ=2), thus occurring an increase in the synthesis temperature that provided greater sintering between the particles, resulting in more porous flakes in relation to the stoichiometric amount of fuel synthesis. These morphological characteristics are the result of the effervescence in the combustion process combined with the short reaction time, preventing the growth of particles [26]. In addition, these nanostructured flakes are interesting for various applications. Table I shows the results of the specific surface area (S_{BET}) of the crushed samples. The phosphors synthesized with the stoichiometric amount of urea (φ=1) had an S_{BET} of 0.15 m^2/g due to a nanostructured flake shape formed by the union between particles as seen in Fig. 3a after efficient combustion. The sample obtained with excess urea (φ=2) showed an S_{BET} of 0.07 m^2/g showing that increasing fuel resulted in greater sintering of this product, leading to the formation of agglomerations and consequently reducing the S_{BET} of the product [24].

Optical characterization: in the crystal lattice of $Sr_3Al_2O_6$, there were six possible sites to accommodate Eu by taking place of Sr. The analysis based on the effective bond valence theory showed that the active valence of Sr in each site was different. Eu entered into the different sites of Sr, thus, the energy barrier that Eu had to overcome was different, since the coordination number and the average length of neighboring-coordination bonds for each site of Sr were different. Accordingly, the reduction-ability of the Eu was diverse depending on its site occupation. If all Eu ions were completely reduced to Eu^{2+}, it would emit green luminescence [27]. Despite the contradictory results for $Sr_3Al_2O_6$ doped with europium, the observed differences in emission spectra are caused by differences in excitation wavelengths and different crystallographic sites for Eu^{2+} and Eu^{3+} as were explained by Huang et al. [28] and Zhang et al. [29] and also due to the coexistence of Eu^{2+} and Eu^{3+} in the samples. In order to see Eu^{3+} contribution, the emission spectra of samples with the stoichiometric amount of urea (φ=1, green open circles) and with the excess of fuel (φ=2, blue open squares) were taken under 464 nm excitation as shown in Fig. 4a. The 464 nm was chosen to be the excitation wavelength, taking in account the results obtained in excitation spectrum fixing the emission at 611 nm (Fig. 4b). For the emission wavelength at 611 nm, the transitions at $^7F_{0,1}$-$^5D_2$ are clearly seen at 464 nm [9]. As seen in Fig. 4b, the strongest peak is located at 464 nm. Effectively, the emission intensity centered at 611 nm increased in the sample with lower fuel content due to the lack of reduction of europium. If Eu^{3+} was completely reduced to Eu^{2+}, it would give green luminescence in the crystal lattice of $Sr_3Al_2O_6$ and the excitation and emission originate from the real $4f^7$-$4f^65d$ transition of Eu^{2+} [27].

The excitation spectra fixing the emission at 515 nm are shown in Fig. 5a for the samples with the stoichiometric amount of urea (φ=1, green open circles) and with the excess of fuel (φ=2, blue open squares) showing a broad band in UV range with the maxima around 365 nm. The emission spectrum of the sample with φ=1 under 365nm excitation is shown in Fig. 5b. The emission band centered at 425 nm can be assigned to an anomalous Eu^{2+} trapped exciton emission [6] and the emission bands located at 588, 596, and 611 nm corresponded to the transition of $^5D_0 \rightarrow {}^7F_1$,

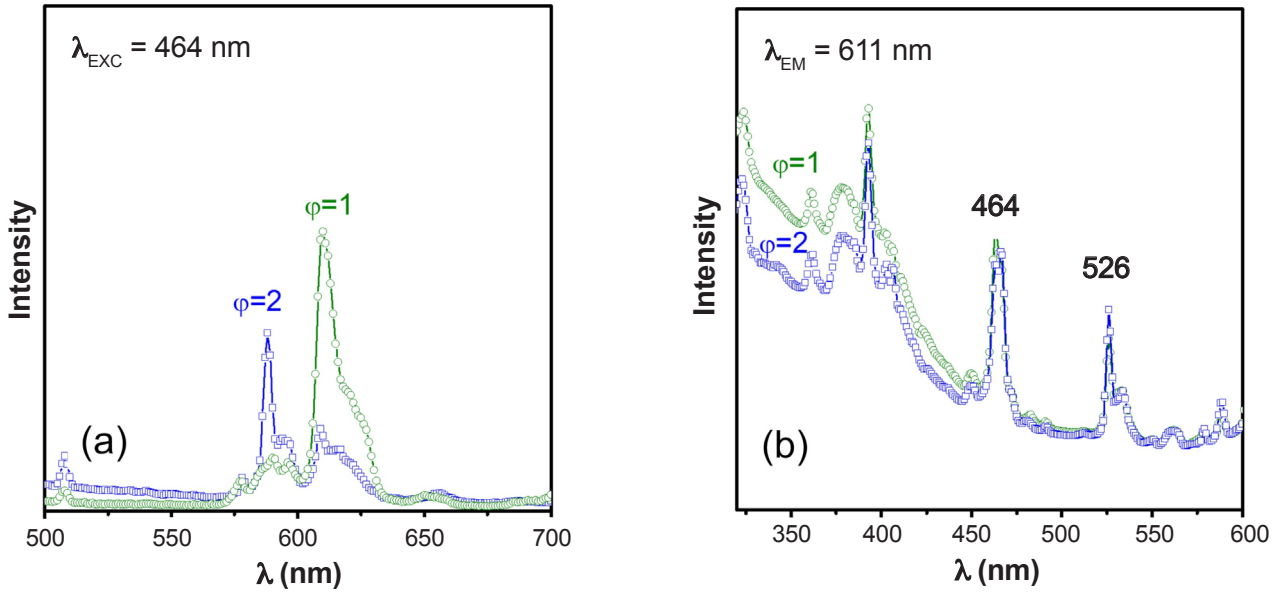

Figure 4: Emission spectra of the samples with the stoichiometric amount of urea (φ=1) and with the excess of fuel (φ=2) under 464 nm excitation (a), and excitation spectra of the samples with φ= 1 and 2 fixing the emission at 611 nm (b).

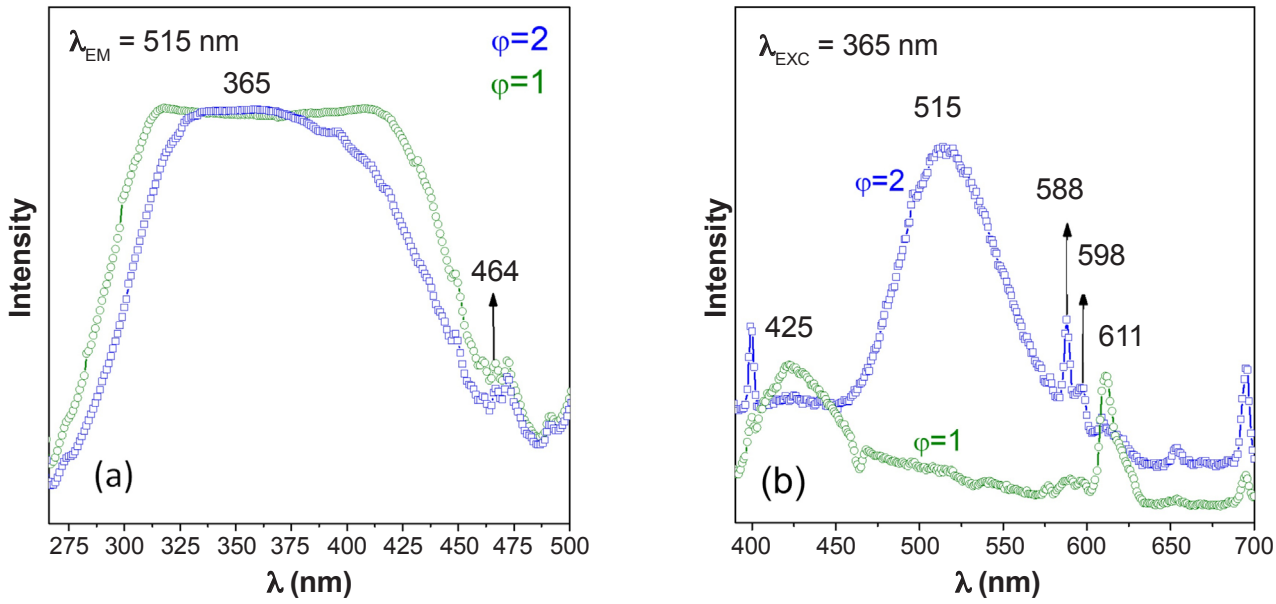

Figure 5: Excitation spectra of the samples with the stoichiometric amount of urea (φ=1) and with the excess of fuel (φ=2) fixing the emission at 515 nm (a), and emission spectra of the samples with φ= 1 and 2 under 365 nm excitation (b).

$^5D_0 \rightarrow {}^7F_1$, and $^5D_0 \rightarrow {}^7F_2$ for the Eu^{3+} ions, respectively [27, 30-32]. The emission spectrum of the sample with φ=2 is shown also in Fig. 5b. The emission band centered at 515 nm was assigned to the transition of $4f^65d^1/4f_7(^8S_{7/2})$ of Eu^{2+} ions and the emission bands located at 588, 598, and 611 nm corresponded to the transition of $^5D_0 \rightarrow {}^7F_1$, $^5D_0 \rightarrow {}^7F_1$, and $^5D_0 \rightarrow {}^7F_2$ for the Eu^{3+} ions, respectively. The emission at 611nm was more relevant in the sample with the stoichiometric amount of urea (φ=1) than in the sample with the excess of fuel (φ=2). It is important to remark that the combustion method avoids the use of a reducing atmosphere during the thermal treatment due to fuel burnout, a creation of suitable atmospheric conditions to reduce the Eu^{3+} to Eu^{2+} [18]. For this reason, the intensity of the peaks corresponded to Eu^{3+} decreased for φ=2. However, there was not a total reduction of Eu^{3+}. The results indicated that the excitation spectrum (Fig. 5a) of the sample with the excess of fuel (φ=2) had a peak position in the band from 275 to 475 nm corresponding to the crystal field splitting of the Eu^{2+} d-orbital, being located in the main peak at 365 nm under an emission of 515 nm, which meant that it can be effectively excited by ultraviolet light.

During the last few years, a number of publications have appeared on the luminescence properties of Eu^{2+} in $Sr_3Al_2O_6$. The reported results concerning the position of Eu^{2+} emission in $Sr_3Al_2O_6$:1% Eu^{2+} are confusing or even in contradiction to each other [6]. Some authors [33-35] have reported green emission of $Sr_3Al_2O_6$:Eu^{2+} peaking around 510 nm, under 360 nm excitation. Other authors [36] reported broad green band emission but peaking at 518 nm. Studies have shown a broad red emission peak at 604 nm under the excitation wavelength of 460 nm [29]. Additionally, emissions at 405 and 435 nm from $Sr_3Al_2O_6$:Eu^{2+} have been reported [37]. The differences in emission spectra of $Sr_3Al_2O_6$:Eu^{2+} are caused by differences in excitation wavelengths [28]. The green and red emissions originate from different crystallographic sites for Eu^{2+}. The $Sr_3Al_2O_6$:Eu^{2+}/Dy^{3+} phosphor emits a yellow-green light upon UV illumination and bright red light upon visible light illumination. The peak positions in the emission spectra depend strongly on the nature of the Eu^{2+} surroundings, and therefore, Eu^{2+} ions can emit different visible lights in the various crystal fields [38]. According to Zhu et al. [39], the red luminescence of $Sr_3Al_2O_6$:Eu could be improved by doping with Dy^{3+} and be further improved by co-doping with Li^+. As also, there is a correlation between the luminescent responses of the materials processed in the presence of the oxidizing agent. The higher fuel content produces different Eu^{2+}/Eu^{3+} ratios that account for photoluminescence centered at different wavelengths.

CONCLUSIONS

By solution combustion synthesis method avoiding thermal treatments in a reducing atmosphere, $Sr_3Al_2O_6$:Eu phosphors were successfully synthesized. The amount of urea had an important influence on the luminescence response; a urea content larger than the stoichiometric one required the presence of an oxidant agent such as HNO_3 to complete the reaction. The synthesized phosphor showed an intense band emission centered at 515 nm. The optical properties correlated with the Eu^{2+}/Eu^{3+} ratio and their emissions. Particles having nanostructured flake-type morphology were obtained. The combustion method avoided the standard requirements of post-thermal treatments in a reducing atmosphere to promote the appearance of Eu^{2+} cations. The fuel content had two roles: the effective chelation of the cations and the creation of suitable atmospheric conditions to reduce the Eu^{3+} to Eu^{2+}. The optimized synthesis and processing conditions by the solution combustion method in presence of oxidizing agent provided a micro-nanofunctional

candidate for practical applications.

ACKNOWLEDGEMENTS

This work was supported by the Ministry of Economy and Competitiveness of Spain under project MAT2013-48426-C2-1R and the Brazilian Program "Science Without Borders" through Project Nº 401220/2014-1. The financial support from the Estonian Research Council (grant PSG-466) is gratefully acknowledged by R.E Rojas- Hernandez.

REFERENCES

[1] G. Balachandran, Treat. Process Metall. **3** (2014) 1291.
[2] I. Gupta, S. Singh, S. Bhagwan, D. Singh, Ceram. Int. **47** (2021) 19282.
[3] S.K. Gupta, R.M. Kadam, P.K. Pujari, Coord. Chem. Rev. **420** (2020) 213405.
[4] V.B. Pawade, S.J. Dhoble, Luminescence **26** (2011) 722.
[5] X. Li, Y. Liang, F. Yang, Z. Xia, W. Huang, Y. Li, J. Mater. Sci. Mater. Electron. **24** (2013) 3199.
[6] D. Dutczak, T. Jüstel, C. Ronda, A. Meijerink, Phys. Chem. Chem. Phys. **17** (2015) 15236.
[7] J. Qi, X. Zhang, X. Han, Y. Li, X. Wu, R. Zhong, R. Guo, J. Alloys Compd. **678** (2016) 421.
[8] P. Zhang, L. Li, M. Xu, L. Liu, J. Alloys Compd. **456** (2008) 216.
[9] P. Page, R. Ghildiyal, K.V.R. Murthy, Mater. Res. Bull. **41** (2006) 1854.
[10] A.H. Wako, F.B. Dejene, H.C. Swart, Phys. B Condens. Matter. **480** (2015) 116.
[11] P. Ptácek, in "Strontium aluminate: cem. fundam. manuf. hydration, setting behav. appl.", IntechOpen (2014) 236.
[12] B. Farin, A.H.A. Monteverde Videla, S. Specchia, E.M. Gaigneaux, Catal. Today **257** (2015) 11.
[13] Y. Xu, Y. He, X. Yuan, Powder Technol. **172** (2007) 99.
[14] P. Zhang, M. Xu, Z. Zheng, B. Sun, Y. Zhang, Trans. Nonferrous Met. Soc. China **16** (2006) s423.
[15] P. Zhang, M. Xu, L. Liu, L. Li, J. Sol-Gel Sci. Technol. **50** (2009) 267.
[16] M.A. Aghayan, M.A. Rodríguez, Mater. Sci. Eng. C **32** (2012) 2464.
[17] A.S. Mukasyan, P. Epstein, P. Dinka, Proc. Combust. Inst. **31** (2007) 1789.
[18] R.E. Rojas-Hernandez, M.A. Rodriguez, J.F. Fernandez, R. Soc. Chem. **5** (2015) 3104.
[19] M. Kavitha, R. Subramanian, K.S. Vinoth, R. Narayanan, G. Venkatesh, N. Esakkiraja, Powder Technol. **271** (2015) 167.
[20] S.R. Jain, K.C. Adiga, V.R. Pai Verneker, Combust. Flame **40** (1981) 71.
[21] W.T. Barbosa, I.V.S.R. Nascimento, R. Garcia-Carrodeguas, M.V.L. Fook, M.A. Rodríguez, Int. J. Appl. Ceram. Technol. **16** (2019) 595.
[22] F. Hanic, T.Y. Chemekova, Y.P. Udalov, Zh. Neorg. Khim. **24** (1979) 471.
[23] R. Ianoş, R. Istratie, C. Păcurariu, R. Lazău, Phys. Chem. Chem. Phys. **18** (2016) 1150.
[24] M.A. Rodríguez, C.L. Aguilar, M.A. Aghayan, Ceram. Int. **38** (2012) 395.
[25] R.E. Rojas-Hernandez, M.A. Rodriguez, F. Rubio-Marcos, A. Serrano, J.F. Fernandez, J. Mater. Chem. C **3** (2015) 1268.
[26] L.L. Petschnig, G. Fuhrmann, D. Schildhammer, M. Tribus, H. Schottenberger, H. Huppertz, Ceram. Int. **42** (2015) 4262.
[27] L. Chen, Z. Zhang, Y. Tian, M. Fei, L. He, P. Zhang, W. Zhang, J. Rare Earths **35** (2017) 127.
[28] P. Huang, Q. Zhang, C.E. Cui, J. Li, Opt. Mater. **33** (2011) 1252.
[29] J. Zhang, X. Zhang, J. Shi, M. Gong, J. Lumin. **131** (2011) 2463.
[30] X. Li, H. Pan, A. Tang, J. Zhang, L. Guan, H. Su, G. Dong, Z. Yang, H. Wang, F. Teng, J. Nanosci. Nanotechnol. **16** (2016) 3474.
[31] K. Binnemans, Coord. Chem. Rev. **295** (2015) 1.
[32] J.A. Capobianco, P.P. Proulx, M. Bettinelli, F. Negrisolo, Phys. Rev. B **42** (1990) 5936.
[33] C. Chang, W. Li, X. Huang, Z. Wang, X. Chen, X. Qian, R. Guo, Y. Ding, D. Mao, J. Lumin. **130** (2010) 347.
[34] D. Gingasu, I. Mindru, A. Ianculescu, S. Preda, C. Negrila, M. Secu, J. Lumin. **214** (2019) 116540.
[35] Y. Li, Y. Wang, Y. Xiong, T. Peng, M. Mo, J. Rare Earths **30** (2012) 105.
[36] A. Yu, D. Zhang, Y. Hu, R. Yang, J. Mater. Sci. Mater. Electron. **25** (2014) 4434.
[37] D. Si, B. Geng, S. Wang, CrystEngComm **12** (2010) 2722.
[38] P. Huang, C.E. Cui, S. Wang, Opt. Mater. **32** (2009) 184.
[39] M. Zhu, Y. Tian, J. Chen, M. Fei, L. He, L. Chen, F. Peng, Q. Zhang, T.-S. Chan, Funct. Mater. Lett. **11** (2018) 1850012.
(Rec. 11/07/2022, Rev. 18/10/2022, Ac. 25/10/2022)